



UWS Academic Portal

Pelton turbine bucket flow analysis and visualization for evaluation of area-wise contribution

Bhattarai, S.; Vichare, P.; Dahal, K.

Published in:
Renewable and Sustainable Energy Developments Beyond 2030

Published: 08/05/2018

Document Version
Publisher's PDF, also known as Version of record

[Link to publication on the UWS Academic Portal](#)

Citation for published version (APA):
Bhattarai, S., Vichare, P., & Dahal, K. (2018). Pelton turbine bucket flow analysis and visualization for evaluation of area-wise contribution. In A. G. Olabi (Ed.), *Renewable and Sustainable Energy Developments Beyond 2030: Proceedings of the 11th International Conference on Sustainable Energy & Environmental Protection* (Vol. 3, pp. 367-372). Paisley: University of the West of Scotland.

General rights

Copyright and moral rights for the publications made accessible in the UWS Academic Portal are retained by the authors and/or other copyright owners and it is a condition of accessing publications that users recognise and abide by the legal requirements associated with these rights.

Take down policy

If you believe that this document breaches copyright please contact pure@uws.ac.uk providing details, and we will remove access to the work immediately and investigate your claim.



UWS UNIVERSITY OF THE
WEST of SCOTLAND

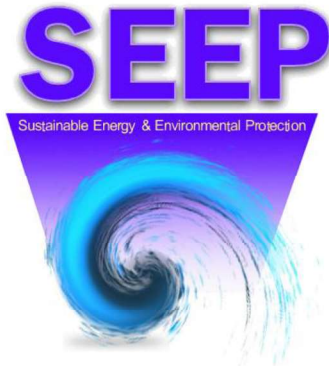
Institute of Engineering and
Energy Technologies

RENEWABLE AND SUSTAINABLE ENERGY DEVELOPMENTS BEYOND 2030

VOLUME 3

SEEP CONFERENCE 2018

University of the West of Scotland, Paisley Campus
Tuesday 8-Friday 11 May 2018



Renewable and Sustainable Energy Developments Beyond 2030

VOLUME 3

*Proceedings of the  International Conference on
Sustainable Energy & Environmental Protection*

EDITED BY:

Prof Abdul Ghani Olabi

University of the West of Scotland

School of Engineering & Computing

Institute of Engineering & Energy Technologies

© Abdul Ghani Olabi 2018

“Renewable and Sustainable Energy Developments Beyond 2030

VOLUME 3”

First Published in 2018

by

University of the West of Scotland

High Street, Paisley, PA1 2BE

UK

The authors have asserted their moral rights

ISBN: 978-1-903978-62-7

All rights reserved.

Table of Contents

Air quality

Impacts of elevated point sources emissions on air quality using an Eulerian on-line model R.S. José, J.L. Pérez, L. Pérez, R.M. Gonzalez	1
Impact of power plants on the ambient air quality of Kuwait Ahmed Z. Aly, Fahad M. Al-Fadhli, Nawaf S. Alhajeri, Andrew Reimers, and Michael E. Webber.....	7
Factors affecting public risk perception of air pollution in China Lingling Wang and Tsunemi Watanabe.....	13
The status quo and current trends of energy-related carbon dioxide emissions in Malaysia, based on LMDI decomposition method Chinhao Chong, Weixin Tan, Zhaoji Ting, Linwei Ma, Weiqi Lib, Geng Kong, Zheng Li,..	17
Particle size influence on hazard gases emission of bituminous coal spontaneous combustion during high temperature J.Y. Zhao, Y.N. Zhang, J. Guo, X.Z. Zheng, and C.M. Shu.....	23
A quantitative assessment of electric power system contributions to atmospheric pollutants in Kuwait Nawaf S. Alhajeri, Fahad M. Al-Fadhli, Ahmed Z. Aly, Andrew Reimers and Michael E. Webber.....	29

Battery and Energy Storage

Synthesis and physical / electrochemical characterisation of Nitrogen-doped Carbon /activated carbons as an excellent electrode material for electrochemical capacitor applications Qaisar Abbas and Mojtaba Mirzaeian	35
Battery thermal management system with liquid cooling and phase change material Ziye Ling, Jiahao Cao, Zhengguo Zhang, Xiaoming Fang, Xuenong Gao	41
Investigation of the thermal behaviour of high-capacity lithium ion batteries R. Rizk, H. Louahlia, H. Gualous and P. Schaezel	47
Life cycle assessment of lithium-ion traction battery: discussion on methodology development and GHG emissions performance Siqin Xiong and Xiaoming Ma	53
Dynamic model supported approach for battery system selection in the transformer substation K. Deželak and J. Pihler.....	59
A review on critical aspects of lithium-ion battery overcharge Yi-Hong Chung, Anjani R.K. Gollakota, Wei-Chun Chen, Yih-Wen Wang, Chi-Min Shu...65	

On-board state-of-health estimation of lithium-ion battery based on grey relational analysis method Xiaoyu Li1, Zhenpo Wang	71
Optimum design and hierarchical control for PV/Hydrogen/Battery-based dc micro grid Ying Han, Qi Li, Weirong Chen, Firuz Zare, Guorui Zhang.....	77
Thermal assessment of constor rbmk-1500 casks during long-term storage of spent nuclear fuel R. Poškas, V. Šimonis, H. Jouhara and P. Poškas.....	83
Multicriteria decision analysis for energy storage technologies coupled to ocean energy systems J. Olmedo González, G. Ramos Sánchez, J. M. Sandoval Pineda, and R de G. González Huerta.....	89
Determining the optimal operation strategy of the energy storage system with the residential photovoltaic system considering electricity usage and profits Seunghoon Jung, Taehoon Hong, Hyuna Kang, Minhyun Lee, Kwangbok Jeong.....	95
Thermo-economic study of phase change materials (PCMs) for thermal energy storage Laxman Mishra, Abhijit Sinha, Rajat Gupta.....	101
Energy Development and Storage	
Development of a global energy management system for non-energy intensive multi-site manufacturing organisations: implementation overview Noel Finnerty, Raymond Sterling, Daniel Coakley, Sergio Contreras and Marcus M. Keane.....	107
Salinity gradient energy resource in tropical hypersaline coastal lagoons: perspectives for sustainable use. C. Enriquez, O. Reyes-Mendoza, O. Alvarez-Silva, V. Papiol-Nieves, I. Mariño-Tapia, X. Chiappa-Carrara, J. Aragón, N. Fitch and R. Silva-Casarín.....	113
Dynamic analysis of a six-degree of freedom motion wave energy converter based on the concept of the Stewart-Gough platform D.E. Galván-Pozos, F.J. Ocampo-Torres, E. Santiago-Ojeda and M.G. Jaramillo-Torres.....	118
Study on thermal properties and thermal stability of eutectic mixture: CaCl ₂ ·6H ₂ O-NH ₄ Cl-SiCl ₂ ·6H ₂ O as a phase change material for building applications Wanchun Sun, Rongda Ye, Xiaoming Fang, Zhengguo Zhang.....	124
Generation of electrical energy from a salt gradient potential using reverse electrodialysis Rosa de Guadalupe González Huerta, Jesús Nahúm Hernández Pérez, and Arturo M. Robledo.....	130
Advances in OTEC plant prototype for the Mexican Caribbean Sea E. Cerezo, M. Bernal, J.F. Barcenás, M.H. Sánchez, V.M. Romero, M.A. Alatorre and	

R. Silva.....	135
Development of environmental barrier coatings and inherently corrosion resistant composites for the protection and production of components in ocean energy E. López-Honorato, J.M. Mata Padilla, G. Vargas-Gutiérrez, C. Rubio-González and A.R. Hernández-Martínez.....	141
System analysis of energy development in Henan province, china, based on an energy allocation diagram and LMDI decomposition method Geng Kong, Chinhao Chong, Jingjing Liang, Linwei Ma, Zheng Li, Weidou Ni.....	147
Method for estimating embodied energy of construction services based on a DHI/O-SDA model Xi Zhang, Zheng Li, Linwei Ma, Chinhao Chong	153
Investigation of Ternary Carbonates/MgO composite materials for high temperature energy storage Lixia Sang, Feng Li, Yongwang Xu.....	162
An offshore wind turbine mechanical-power electronic coupled fault diagnostic tool J. Mitchell, A. Foley and J. Doran.....	168
Compatible neighbours? – 25 years of spatial wind power development in Germany Marcus Eichhorn, Georgia Erdmann, Jens Ponitka, Magdalena Sachs & Daniela Thrän.....	174
Developments of offshore wind resource assessment for low latitude regions S.N. Uy and A. Alaswad.....	179
Application of numerical weather prediction model for offshore wind resource assessment in the Philippines S.N. Uy and A. Alaswad.....	187
Fuel Cell Technology	
Modelling and simulation of PEM fuel cell flow channel using open pore cellular foam material Tabbi Wilberforce, F. N. Khatib, Ahmed Al Makky, Zaki El-Hassan, A. Baroutaji, A. G. Olabi.....	194
Properties of Nafion/Mordenite composite membrane fabricated by solution-casting method with different solvent ratio Z. H. D1, P. Prapainainar, A. Theampetch and C. Prapainainar.....	204
Effect of humidification of reactive gases on the performance of a Proton Exchange Membrane fuel cell H. Jiang, O. Ijaodola, O. Emmanuel, F.N. Khatib, Tabbi Wilberforce, A.G. Olabi.....	209
Application of the electrophoretic deposition method for the formation of electrode-supported sofc: review of leading edge technologies and on-site experience	

E.Yu. Pikalova, E.G. Kalinina, N.M. Bogdanovich, D.I. Bronin.....	221
Design of experiments analysis of 5 – cell stack fuel cell using three different bipolar plate geometries Tabbi Wilberforce, F. Nisar, Zaki El Hassan, A. G. Olabi.....	227
Influence of mass transfer on electric performance of a unitized regenerative fuel cell during mode switching Q. Guo, H. Guo, F. Ye, C.F. Ma.....	239
CFD model of the effects of non-humidification and humidification of reactant gas on membrane for PEMFC Oluwatosin S. Ijaodola, Abdulrahman Alanazi, Emmanuel Ogungbemi, Tabbi Wilberforce, F.N. Khatib, Ahmed Al Makkay, Zaki El- Hassan, Abdul G. Olabi.....	245
Life cycle assessment of EU critical raw materials in FCH technologies R. Stropnik, M. Sekavčnik, A. Lotrič, M. Mori.....	253
Effect of bipolar plate geometry design on the performance of a Proton Exchange Membrane (PEM) fuel cells Tabbi Wilberforce, A.G. Olabi.....	259
Water Electrolysis Technology F.N Khatib, Tabbi Wilberforce, A. G. Olabi.....	266
Investigation into the effect of thickness in the performance of PEM membrane E.O. Ogungbemi, A. Alanazi, T.A. Wilberforce, O.S. Ijaodola, F. Nisar, A. Al-makky, Zaki El-Hassan, A.G. Olabi.....	276
Facile synthesis and electrochemical properties of silicon oxide-carbon composites using liquid phase plasma process for supercapacitor application W.J. Lee and S.C. Jung.....	281
Fabrication of ultra-thin silicon strain gauge for hydrogen pressure sensor J.-W Choi and J.-S. Kim	287
Overview of hydrogen and fuel cells technology in the aviation sector Ahmad Baroutaji, Tabbi Wilberforce, Abdul Ghani Olabi.....	292
Numerical Modelling	
Electronic differential with extended state observer applied on an electric vehicle system A.B. Ibrahim Farouk Bouguenna, Ahmed Azaiz, Ahmed Tahour, Ahmed Larbaoui.....	298
Numerical investigation on the effect of strut injection system with a cavity based scramjet combustor LakkaSuneetha, Pitambar Rambhau Randive, Krishna Murari Pandey.....	304
Scenario analysis on the substitution for scattered coal by electricity and natural gas based on a dual-objective optimization model in Sichuan province	

Zhou Kui, Li Weiqi, Li Zheng, Chinhao Chong, Linwei Ma.....	310
A numerical approach for the energy efficiency analysis of an entire ceramic tunnel kiln M. Milani, L. Montorsi and M. Venturelli.....	316
Numerical investigation of detonation wave propagation in pulse detonation engine with obstacles Noor Alam, K. M. Pandey, and K. K. Sarma.....	322
Numerical analysis of hydrogen fueled scramjet performance with passive techniques Obula Reddy Kummitha, K.M.Pandey and Rajat Gupta.....	328
Microsimulation of electric vehicle energy consumption Blaž Luin, Stojan Petelin, Fouad Al-Mansour.....	334
A design approach for minimizing subsurface impacts from ground-coupled heat pumps in district scale R.W. Falta, F.J. Molz, and C.J. Newell.....	343
Laminar burning velocities of CH ₄ /CO/O ₂ /CO ₂ mixtures Yongliang Xie and Xujiang Wang.....	348
Observed model predictive control of a two-body point absorber wave energy converter H.E.M. Triki, E. Bdirina and M.S. Lagoun.....	354
Experimental and numerical investigation on the effects of low pressure cooled EGR on knock tendency and performance of a downsized turbocharged SI engine C. Tornatore, F. Bozza, V. De Bellis, L. Teodosio, G. Valentino, L. Marchitto.....	360
Pelton turbine bucket flow analysis and visualization for evaluation of area-wise contribution S. Bhattarai, P. Vichare and K. Dahal.....	367
Reliability modelling of flywheel energystorage system for power system operational reliability assessment Saket Adhikari and Rajesh Karki.....	373

PELTON TURBINE BUCKET FLOW ANALYSIS AND VISUALIZATION FOR EVALUATION OF AREA-WISE CONTRIBUTION

S. Bhattarai, P. Vichare and K. Dahal

School of Computing and Engineering, University of the West of Scotland, Paisley, UK; email:

suyesh.bhattarai@uws.ac.uk, parag.vichare@uws.ac.uk, keshav.dahal@uws.ac.uk.

ABSTRACT

The objective of this paper is to visualize, evaluate and analyse the flow in a Pelton turbine bucket. The numerical study of the buckets in rotating condition allows for detailed study and analysis of the jet-bucket interaction from the moment of impingement to the moment of exit. Unsteady numerical simulations, based on two phase homogenous model, was performed for wall pressure measurement and flow visualization. Realizable K-epsilon viscous model with near wall treatment was used for turbulence modelling. Similar studies have been conducted for the inner bucket surface and are limited to verifying the experimental and numerical results. This study extends the research to the chronologic performance of specific segments inside the bucket; on the reverse side of the bucket and the edges. It attempts to expose the most and the least efficient parts of the bucket so that the designers can contemplate better designs to enhance the performance. The research suggests that the splitter area and the central base region of the bucket are the most productive whereas the portion at the root; and at the outer periphery is the least productive.

Keywords: Pelton turbine, Computational fluid dynamics, Flow analysis, Design analysis.

1 INTRODUCTION

Pelton turbine is a technology that has been used in simple form as water wheels for centuries. But due to its complex water jet interactions, detailed study on energy transfer has not been possible. The basic working principle of the Pelton turbine makes it susceptible to bucket reverse side splashing, atomization of the jet, interference of water layers, secondary flow within the jet and gravity deviation of the water etc. which play a major role in energy loss in the turbine [1]. In such conditions, obtaining accurate measures of energy that can be generated from the turbine based on analytical methods alone is a humungous task. The CFD methods utilize the processing capabilities of the computers that can help study the water-bucket interaction in detail. This detailed evaluation and visualization allows for inspection of chronological contribution of the different areas of the Pelton bucket.

This paper presents the CFD results of Pelton bucket flow analysis with respect to time for each of the contribution areas identified in the bucket. The second section presents related work in this area, and the third section details the methodology used for conducting the simulation which is rarely available in other literature. The fourth section provides the results and critical discussion based on the results while the fifth section provides the conclusion for the entire study.

2 RELATED WORK

The literature available on Pelton turbine performances ranges from investigating the effect of a single bucket feature such as the number of buckets [1] and the angle of attack on the bucket [2] or the length, width, depth, height of the splitter, angle of the splitter, angle of exit, etc. [3] to the effect of the bucket as a whole. There has been a rise in research after the CFD capabilities were proven for free surface flows by the end of the twentieth century. Avellan et. al. in [4] verified the performance of the Volume of Fluid approach used in some of the commercial purpose CFD codes to predict the flow in injectors and bucket geometry of a Pelton turbine.

The environment definition with rotating buckets is more accurate and realistic representation of the problem. But it requires excessive computational capacity and time. In most studies, this computational resource requirement problem has been eased by modelling only three successive buckets [5] or using alternate less accurate methods [6]. The bucket at the middle undergoes the complete cycle of jet entering the bucket and exiting it along with the splashing effects from the previous bucket; hence, it encompasses the all-inclusive cycle of any bucket.

Perrig et al. [7] measured the pressure in the inner surfaces of the buckets using two phase homogenous model. The resultant patterns had a qualitative agreement and a variation of 7-26% was observed in experimental and numerical results. From in-depth analysis, it was concluded that the area near the cut-out

contributed most for the bucket power and the region at the root of the bucket was least productive. This study did not study the edges and the reverse surface of the bucket.

3 METHODOLOGY

Computational fluid dynamics analysis has various aspects for a successful outcome. The different stages and requirements have been highlighted in the subsequent sub-sections.

3.1 Geometric Modelling

Existing design of the Pelton turbine which has been used by many researches as the benchmark was modelled with commercial CAD software and imported into Ansys for pre-processing. The basic details of the turbine assembly are as listed in table 1. Turbine with same features has been used in the studies [3, 8].

Table 1. Basic features of the Turbine [8]

Conditions	Values
Runner Pitch Diameter	400 mm
Jet Diameter	31 mm
Rotation Speed	1150 rpm
Flowrate (nominal)	270.6 m ³ /h
Net head	129.6 mWG
Buckets	22
Injectors	1
Power Output (2x nominal flowrate)	80.14 Kw
Torque (2x nominal flowrate)	761.94 Nm

The turbine used by Stamatelos [8] was recreated to be analysed as it provides the detailed geometry and also the experimental results hence, we could replicate the same experiment. These results provide benchmark for validation of the simulation results obtained.

3.2 Environment and Mesh

For further processing only a sector with 4 consecutive buckets were taken with the casing and the injector manifold. This allows reduction of the computational domain and ensures faster runtimes for the simulation and smaller data size.

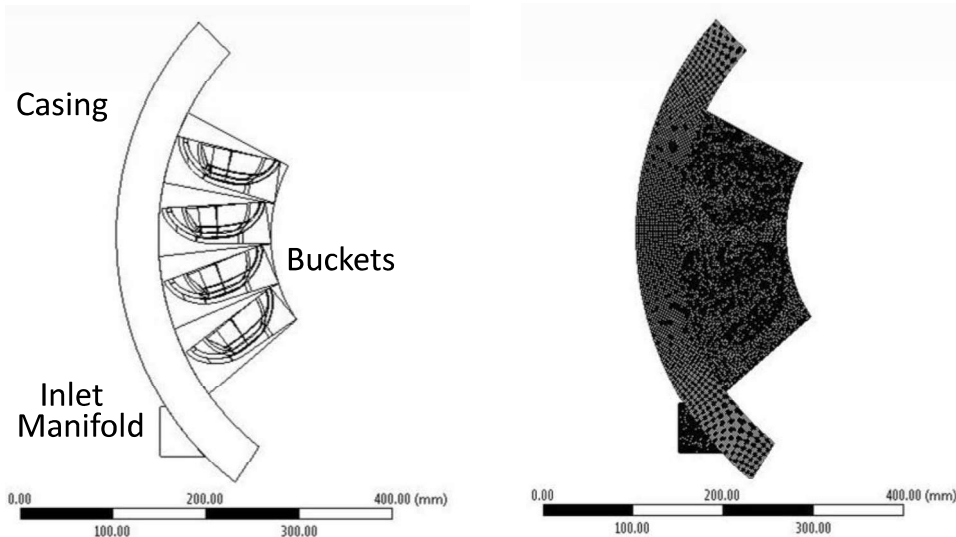


Figure 1. Computational Domain and Mesh

Mesh for the computational domain was generated using Ansys Meshing and best efforts were made to ensure the quality of the mesh. Basic settings used for meshing was of CFD Physics preference and Fluent Solver preference with Fine relevance centre and Element size of 2mm. Patch Independent Tetrahedral Mesh was used for meshing the buckets as it was demanding to generate a Hexahedral Mesh for an irregular surface such as a bucket profile. Table 2 shows the element count for the mesh and the various attributes of the mesh that determines its quality and in turn its accuracy.

Table 2. Mesh Attributes

Parameters	Values		
	Min	Max	Average
Nodes	409306		
Elements	934034		
Aspect Ratio	1.0041	46.678	1.6851
Element Quality	0.0296	0.9999	0.8691
Orthogonal Quality	0.0398	0.9997	0.8861
Skewness	0.00001	0.96636	0.1850

The number of nodes was limited as Academic Researcher Licence of Ansys Fluent was being used. The mesh attributes have been kept well in check with great difficulty. The Aspect ratio and Skewness although acceptable was very difficult to handle as the environment had a lot of curved surfaces.

3.3 Solver

After the pre-processing, the generated mesh was loaded in the Fluent solver environment. The Pressure Based Transient solver was chosen with the Multiphase Volume of Fluid model and Realizable K-epsilon viscous model as basic settings for Fluent environment. The details of the solver scheme are listed below in table 3.

Table 3. Fluent Settings

Description	Mode
Solver Type	Pressure Based
Time	Transient
Model	Multiphase Volume of Fluid
Viscous Model	Realizable K-epsilon
Scheme	Simplec
Spatial Discretization Gradient	Least Squares Cell Based
Pressure	PRESTO!
Momentum	Second Order Upwind
Time Stepping Method	Fixed
Time Step Size	2e-5 s
Number of Time Steps	400

Fixed time stepping with the time step size of 2e-5s was used to keep the Courant Number in check. The boundary conditions were defined in such a way that it resembled the actual working conditions. The net head was used as the gauge pressure for the inlet and the inlet flow rate for primary phase Air, was set at zero as only water flows through the inlet.

3.4 Boundary Conditions

Boundary conditions as listed in table 4 were applied to replicate the realistic working environment.

Table 4. Boundary Conditions

Parameters	Details
Net head	129.6 mWG
Inlet Water Flow Rate	37.9491 kg/s
Inlet Air Flow Rate	0 kg/s
Turbine RPM	120.427 rad/s
Rotation Axis	Z
Outlet	Atmospheric Pressure Outlet
Walls	Movement relative to adjacent cell zone

4 RESULTS AND DISCUSSION

To study the impact of different parts of the bucket surface to the overall power output, the bucket surface was divided into 27 different zones. There were 9 zones on the inside of the bucket, 7 zones on the edges, 10

zones on the back and the cut-out. This division made it easier to obtain localized data for the zones and evaluate their overall performance. The division of zones is illustrated in figure 2.

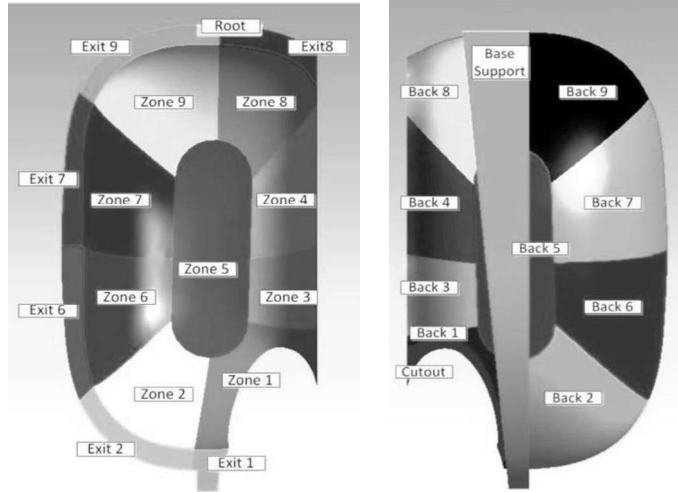


Figure 2. Zone division on bucket surface

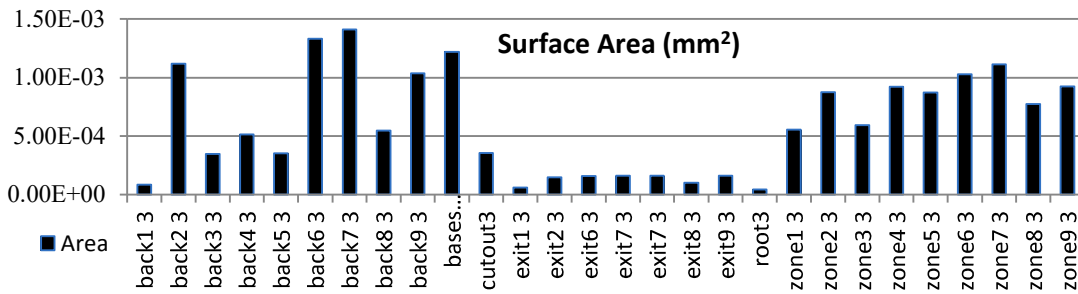


Figure 3. Surface area comparison of different zones

All the zones do not represent equal surface area hence, the surface area of each zones was measured to evaluate the total force experienced by each zone. The area represented by each zone is illustrated in figure 3. The naming convention followed for each zone is the zone name followed by the bucket number. Back1 3 means it is the zone back1 of bucket number 3. Calculations have been made only for this bucket as it undergoes the entire cycle of back splashing to the jet leaving the bucket.

4.1 Inner Surface

The pressure readings and the respective forces generated with respect to time are represented in the graphs below. The first set of graph represents the pressure respective forces on the internal zones of the bucket profile. The readings show that Zone 5 and Zone 3 are the most productive zones on the bucket surface. Zone 2 and Zone 8 are the least productive regions of the bucket as they experience the least pressure from the jet and hence exert the least force and torque to the overall system. Other internal zones are moderately productive.

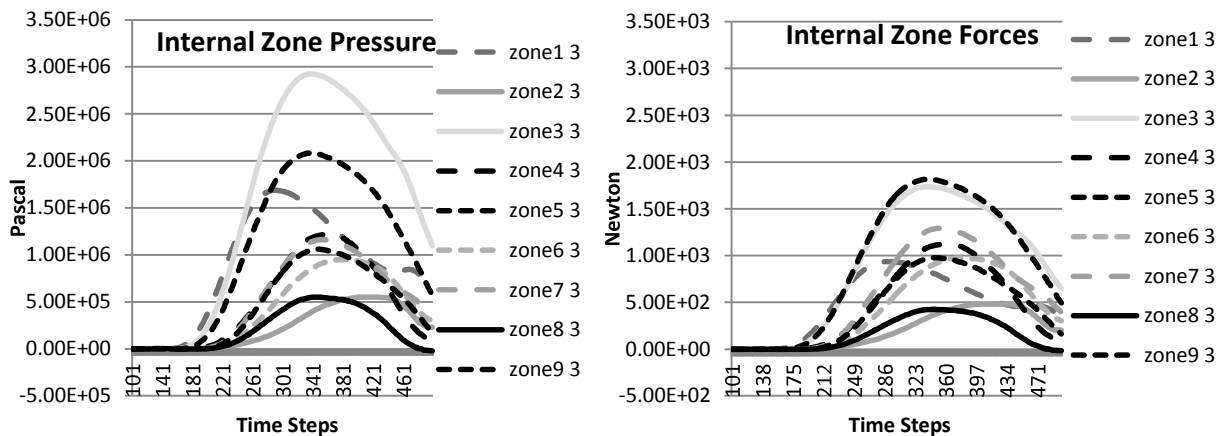


Figure 4. Pressure and Forces on Internal Zones

4.2 Reverse Surface

The back surfaces collectively share more surface area than the internal zones. These zones are expected to experience minimal force on them. But Back 7 and Back 9 experience some considerable amount of force on them which acts the counter force to the system. This force should be kept to a minimum to ensure maximum productivity of the system. This is because of splashing effect from the jet that was reflected from the preceding bucket.

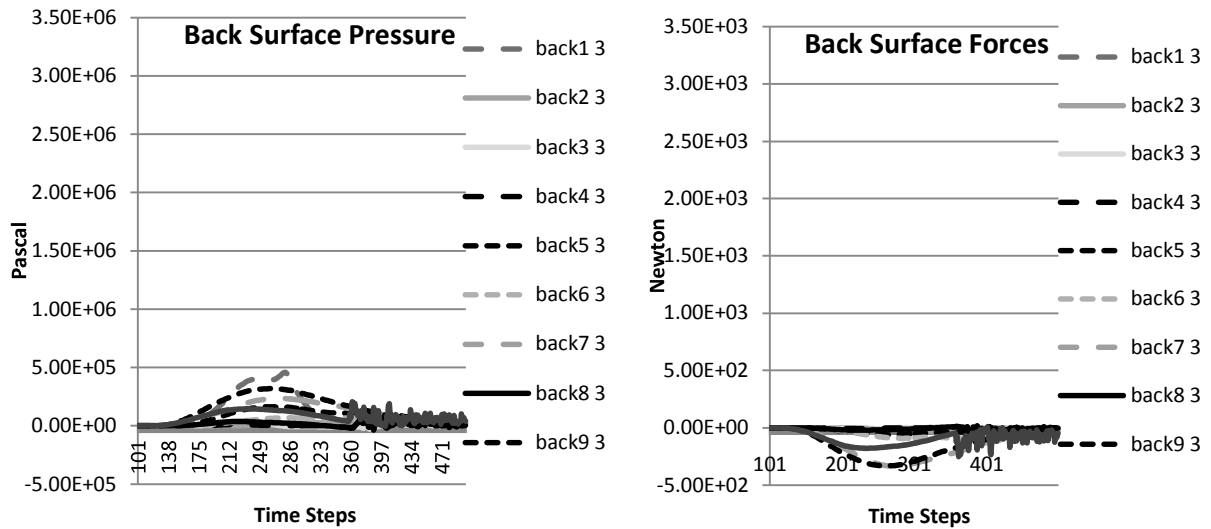


Figure 5. Pressure and Forces on Back Surfaces

4.3 Edges and Cut-out

The next set of graphs represents the readings for the cut-out and the exits. These are the borderline regions that do not cover a wide area. The cut-out is the portion where the jet first interacts with the bucket and although it represents a small area, it experiences considerable pressure and adds to the total force generated. It is almost as productive as the zones 2 and 8 although it has much lower surface area. But the force generated is for a smaller time period as the jet does not interact with this surface for a longer time. Also, effort must be made to reduce this surface area as more interaction with this area leads to less interaction with the internal zones which are more productive than the cut-out.

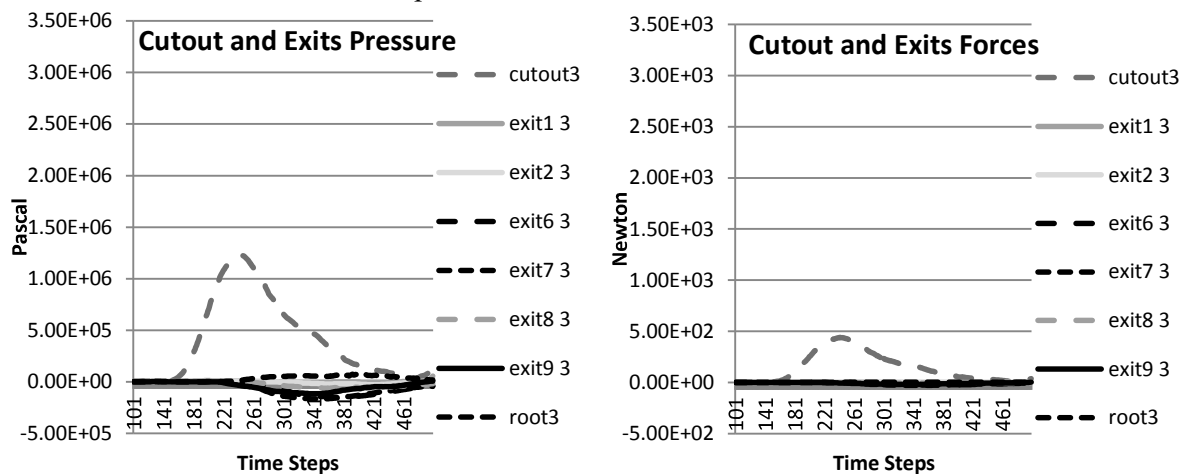


Figure 6. Pressure and Forces on Cut-out and Exits

The above analysis reveals that there are some zones on the surface of the bucket such as Zone 2, Zone 8, the Cut-out, Back 7 and Back 9 that need special attention while considering changes in design for optimization. Also, since the Exit areas do not seem to be adding much to the productivity, using much narrower exits can be considered to reduce the material required for fabrication. This would help reduction of the weight of the wheel and its material cost.

Fluent is an Eulerian method based solver for CFD problems. Although it has high accuracy, it requires long time and high computational power to obtain the final solution. This simulation took roughly 48 hours to

complete not accounting for the geometric modelling and pre-processing part. Following table shows the comparison of results obtained from experiments and the simulation conducted. The accuracy of 0.46% achieved is of a very high order although such simulations usually have an error range of 10-12%. This calculation validates the approach used in this study.

Table 5. Experimental and Simulated results

Parameters	Values
Input Power to turbine	91.93 kW
Power Output (Analytical)	80.14 kW
Torque (Fluent)	766 Nm
Torque (Analytical)	761.94 Nm
Error	0.4699%

5 CONCLUSION

This study was conducted to research the chronological contribution of different zones in the Pelton bucket with a view to identify the most productive and the least productive regions of the bucket. The simulation results show that the inner zones 3 and 5 are the most productive zones. The inner zones 2 and 8 are the least productive as they have similar force contribution as the cut-out which only has half their surface area. Hence, future studies could be concentrated on increasing the areas with profile similar to inner zones 3 and 5; and reducing areas with profile similar to inner zones 2 and 8. The reverse surface zones 7 and 9 experience reverse surface splashing which can be reduced by adjusting the exit angle at the bucket zones 7 and 9. Incorporating these changes to the design of the existing bucket could enhance its efficiency. The simulation conducted in this study has been validated with the experimental results and analytical calculations for same turbine in same flow conditions. The total torque measurement had an error of 0.4699% which confirms the authenticity of the simulations carried out. This study provides insight for the researchers on the contribution of the various zones in the Pelton bucket and provides suggestions for improvement of the efficiency of the bucket by making some design changes.

ACKNOWLEDGEMENTS

The first author likes to acknowledge the support provided by the EU Erasmus Mundus project SmartLink (552077-EM-1-2014-1-UK-ERA) to carry out this research at the University of the West of Scotland, UK.

REFERENCES

- [1. Zidonis, A. and G. Aggidis, *Pelton turbine: identifying the optimum number of buckets using CFD*. Journal of Hydrodynamics, 2015.
- [2. Shogenji, K. and T. Inada, *On the Inclination of the Ridge of Buckets on a Pelton Wheel*. Memoirs of the College of Engineering 1927. **4**(7): p. 339-352.
- [3. Zidonis, A., et al., *Parametric Optimization of Two pelton Turbine Runner Designs Using CFD*. Journal of Hydrodynamics, 2014. **27**(3): p. 403-413.
- [4. Avellan, F., et al. *Flow calculations in Pelton Turbines, Part 2: Free Surface Flows*. in *Proceedings of the 19th IAHR Symposium*. 1998. Singapore.
- [5. Rossetti, A., et al., *Influence of the Bucket Geometry on the Pelton Performance*. Journal of Power and Energy - Proceedings of the institution of Mechanical Engineers, 2014. **228**: p. 33-46.
- [6. Bhattarai, S., P. Vichare, and K. Dahal, *Performance Comparison of Adapted Delaunay Triangulation Method over NURBS for Surface Optimization Problems*, in *The 31st Annual European Simulation and Modelling Conference*, P.J.S. Goncalves, Editor. 2017, EUROSIS-ETI: Lisbon. p. 76-80.
- [7. Perrig, A., et al., *Flow in a Pelton Turbine Bucket: Numerical and Experimental Investigations*. Journal of Fluids Engineering, 2006. **128**: p. 350-359.
- [8. Stamatelos, F.G., J.S. Anagnostopoulos, and D.E. Papantonis, *Performance Measurements on a Pelton Turbine Model* Journal of Power and Energy - Proceedings of the institution of Mechanical Engineers, 2010: p. 351-363.

SEEP Conference 2018

University of the West of Scotland, Paisley Campus
Tuesday 8 – Friday 11 May 2018



UWS UNIVERSITY OF THE
WEST *of* SCOTLAND

Institute of Engineering and
Energy Technologies

RENEWABLE AND SUSTAINABLE ENERGY DEVELOPMENTS BEYOND 2030

VOLUME 3

ISBN: 978-1-903978-62-7